inorganics

MDPI

Article

The A-Type $Ln_4N_2S_3$ Series: New Nitride Sulfides of the Light Lanthanoids (Ln = Ce–Nd)

Falk Lissner and Thomas Schleid *

Institut für Anorganische Chemie, Universität Stuttgart, Pfaffenwaldring 55, 70569 Stuttgart, Germany; lissner@iac.uni-stuttgart.de

* Correspondence: schleid@iac.uni-stuttgart.de; Tel.: +49-711-685-64240

Academic Editor: Duncan H. Gregory

Received: 11 November 2016; Accepted: 14 December 2016; Published: 23 December 2016

Abstract: The reaction of lanthanoid metal powders (Ln) with sulfur and cesium azide (CsN_3) as a nitrogen source in the presence of lanthanoid tribromides ($LnBr_3$) yields lanthanoid nitride sulfides with the composition $Ln_4N_2S_3$ (Ln = Ce–Nd) when appropriate molar ratios of the starting material are used. Additional cesium bromide (CsBr) as a flux secures quantitative conversion (7 days) at 900 °C in evacuated silica tubes as well as the formation of black single crystals. All compounds crystallize isotypically with the orthorhombic crystal structure of $La_4N_2S_3$ ($Pnnm$, Z = 2) and their structures were determined from single-crystal X-ray diffraction data ($Ce_4N_2S_3$: a = 644.31(4), b = 1554.13(9), c = 404.20(3) pm; $Pr_4N_2S_3$: a = 641.23(4), b = 1542.37(9), c = 400.18(3) pm; $Nd_4N_2S_3$: a = 635.19(4), b = 1536.98(9), c = 397.85(3) pm). Compared to $La_4N_2S_3$ the a-axes do not fulfill the expectation of the lanthanide contraction. The main feature of the crystal structure comprises N^{3-}-centered $(Ln^{3+})_4$ tetrahedra arranging as pairs $[N_2Ln_6]^{12+}$ of edge-shared $[NLn_4]^{9+}$ units, which are further connected via four vertices to form double chains $^1_\infty\{([NLn_{4/2}]_2)^{6+}\}$. Bundled along [001] like a hexagonal rod packing, they are held together by two crystallographically different S^{2-} anions. Two compounds of a second modification (B-type $La_4N_2S_3$ and $Pr_4N_2S_3$) will also be presented and discussed for comparison.

Keywords: lanthanoid nitride sulfides; dimorphic crystal structures

1. Introduction

The crystal structures of all ternary lanthanide(III) nitride chalcogenides known so far (Ln_3NCh_3, $Ln_4N_2Ch_3$, Ln_5NCh_6, $Ln_{23}N_5Ch_{27}$, and $Ln_{13}N_5Ch_{12}$) and their halide derivatives (Ln_3N_2ChX, $Ln_4NCh_3X_3$, $Ln_5N_2Ch_4X$, $Ln_5N_3Ch_2X_2$, and $Ln_6N_3Ch_4X$; Ln = La–Nd, Sm, Gd–Ho; Ch = S, Se, Te; X = Cl, Br) are dominated by N^{3-} anions in a tetrahedral coordination of Ln^{3+} cations [1–3]. A very interesting structural behavior is exhibited by the nitride chalcogenides with the composition $Ln_4N_2Ch_3$, which occur in seven different crystal structure types. Depending upon the size of both the lanthanide cation (Ln^{3+}) and the chalcogenide anion (Ch^{2-}), some of them differ fundamentally in the linkage of the structure-governing N^{3-}-centered $(Ln^{3+})_4$ tetrahedra. The representatives of the $Sm_4N_2S_3$-type structure [4] crystallize in the monoclinic space group $C2/m$ with Z = 4 and consist of $[NLn_4]^{9+}$ tetrahedra, which share *cis*-oriented edges to form linear strands $^1_\infty\{[NLn_2]^{3+}\}$. In contrast, the linkage via *trans*-oriented edges of $[NLn_4]^{9+}$ tetrahedra builds up undulated chains in the orthorhombic $Ce_4N_2Te_3$-type structure [5] (Ln = La–Nd; $Pnma$, Z = 4), the orthorhombic $Tb_4N_2Te_3$-type structure [6] (Ln = Gd, Tb; $Pnna$, Z = 4), and the monoclinic $Dy_4N_2Te_3$-type structure [6] ($P2_1/c$, Z = 4). As the main structural feature of the orthorhombic A-$La_4N_2S_3$-type structure [7] ($Pnnm$, Z = 2), N^{3-}-centered $(Ln^{3+})_4$ tetrahedra, which first arrange as pairs $[N_2Ln_6]^{12+}$ of two edge-shared $[NLn_4]^{9+}$ units, occur. These are further connected via their four free vertices to form double chains $^1_\infty\{([NLn_2]_2)^{6+}\}$. For the first time, an arrangement of interconnected $[NLn_4]^{9+}$ tetrahedra fused to layers is observed in the monoclinic

$Nd_4N_2Se_3$-type structure [8–11] (*Ln* = La–Nd; *C*2/*c*, *Z* = 4). In these compounds the $[NLn_4]^{9+}$ units are first edge-linked to congonial bitetrahedra $[N_2Ln_6]^{12+}$ again, and they then become cross-connected to $^2_\infty\{[NLn_2]^{3+}\}$ layers via their remaining four free vertices. Finally, a second layered arrangement is found in the monoclinic B-$Pr_4N_2S_3$-type structure [9] (*Ln* = La, Pr; *C*2/*c*, *Z* = 8). In this case, the $[NLn_4]^{9+}$ tetrahedra are first edge-linked to bitetrahedra $[N_2Ln_6]^{12+}$ just like in A-type $La_4N_2S_3$ and $Nd_4N_2Se_3$, but then connected via two vertices to quadruples $[N_4Ln_{10}]^{18+}$, which eventually build up layers $^2_\infty\{[NLn_2]^{3+}\}$ via their four remaining free corners. In addition, there are only two compounds crystallizing dimorphously so far. $La_4N_2S_3$ [7,12] is found in the A-$La_4N_2S_3$- and in the B-$Pr_4N_2S_3$-type structures, while $Ce_4N_2Se_3$ is observed either with the $Nd_4N_2Se_3$- or with the $Ce_4N_2Te_3$-type arrangement.

2. Results and Discussion

The members of the short $Ln_4N_2S_3$ series (*Ln* = Ce–Nd) crystallize orthorhombically in the space group *Pnnm* with two formula units (*Z* = 2) per unit cell (Tables 1–3) and are therefore isotypical with the A-type structure of $La_4N_2S_3$ [7]. Each of the two crystallographically independent Ln^{3+} cations is firstly surrounded by two N^{3-} anions. For $(Ln1)^{3+}$ another four, for $(Ln2)^{3+}$ even four plus one S^{2-} anions appear in their coordination spheres, thus resulting in overall coordination numbers (*C.N.*) of 6 and 6+1. The polyhedron around $(Ln1)^{3+}$ having the site symmetry (*..m*) can be described as a trigonal prism (Figure 1, left), in which both a prism edge (N···N′) as well as the center (*Ln*1) reside on a mirror plane. $(Ln2)^{3+}$, likewise with the site symmetry (*..m*), shows a trigonal prism or octahedron as a coordination polyhedron, which again proves to be very distorted, since it exhibits, in addition, another extra sulfur ligand (S2″) as a cap (Figure 1, right). The distances $d(Ln^{3+}–S^{2-})$ for *Ln* = Ce–Nd start at 283 pm and increase continuously up to a value of 308 pm. For A-type $La_4N_2S_3$ (*a* = 641.98(4), *b* = 1581.42(9), *c* = 409.87(3) pm) [7], the following ligand provides an abrupt increase of distance (*d*(La2–S2″) = 341 pm), but shows an ECoN = 0.26 (effective coordination number [13]); nevertheless, it is a sound contribution to be considered for the whole coordination sphere of $(La2)^{3+}$. In spite of the lanthanide contraction as anticipated, the compounds $Ln_4N_2S_3$ (*Ln* = Ce–Nd) investigated in this work show a remarkable devolution of this mentioned distance *d*(*Ln*2–S2″). First an increase happens from 341 to 351 pm during the transition from the lanthanum to the cerium compound, accompanied by a decreasing ECoN value of 0.13. With the subsequent compounds $Pr_4N_2S_3$ and $Nd_4N_2S_3$, this distance stagnates and finally decreases again to values of 350 and 343 pm (Table 4 and Figure 2, yellow graph), so one can at most speak of a 6+1-fold but never of a real seven-fold coordination for $(Ln2)^{3+}$ (*Ln* = Ce–Nd). This behavior is also repeated in the lattice constants (Table 1 and Figure 2), where in the extreme case an unusual increase of the *a*-axis from the lanthanum to the cerium compound can be observed. The molar volumes V_m monotonically decrease with the increasing atomic number of *Ln*, which finally reflects the lanthanide contraction again.

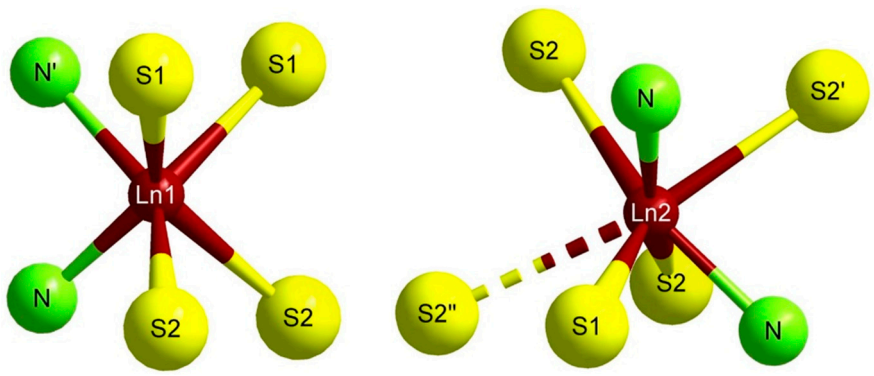

Figure 1. Coordination polyhedra around $(Ln1)^{3+}$ and $(Ln2)^{3+}$ in the A-type crystal structure of the $Ln_4N_2S_3$ series (*Ln* = Ce–Nd).

Table 1. Crystallographic data for the three members of the $Ln_4N_2S_3$ series (Ln = Ce–Nd).

Compound	**$Ce_4N_2S_3$**	**$Pr_4N_2S_3$**	**$Nd_4N_2S_3$**
Crystal system		orthorhombic	
Space group		*Pnnm* (no. 58)	
a/pm	644.31(4)	641.23(4)	635.19(4)
b/pm	1554.13(9)	1542.37(9)	1536.98(9)
c/pm	404.20(3)	400.18(3)	397.85(3)
Z		2	
V_m/cm^3·mol^{-1}	121.87(2)	119.17(2)	116.95(2)
D_x/g·cm^{-3}	5.618	5.772	5.995
Device		Nonius Kappa-CCD (Bruker AXS)	
Radiation		Mo-$K\alpha$ (λ = 71.07 pm)	
$\pm h, \pm k, \pm l$	8, 20, 5	8, 20, 5	8, 20, 5
$2\theta_{max}$/°	56.54	56.60	56.39
F(000)	588	596	604
Absorption correction		numerically (X-SHAPE [14])	
μ/mm^{-1}	22.75	24.88	27.00
Extinction (g)	0.0053	0.0008	0.0007
Measured reflections	9071	7386	6968
Independent reflections	575	552	546
Refl. with $\lvert F_o \rvert \geq 4\sigma(F_o)$	538	457	494
R_{int}, R_σ	0.048, 0.016	0.058, 0.022	0.067, 0.025
Structure solution and refinement		SHELX-97 [15]	
Scattering factors		International Tables, Vol. C [16]	
R_1, R_1 with $\lvert F_o \rvert \geq 4\alpha(F_o)$	0.021, 0.018	0.041, 0.029	0.035, 0.028
wR_2, $GooF$	0.036, 1.174	0.064, 1.100	0.049, 1.166
Resid. electron density ρ_{max}, ρ_{min}/10^{-6} pm^{-3}	1.02, −1.03	1.56, −1.32	1.11, −1.11
CSD numbers [1]	431115	431117	431116

[1] Details of the structure refinements are available at the Fachinformationszentrum Karlsruhe (FIZ), 76344 Eggenstein-Leopoldshafen, Germany (crysdata@fiz-karlsruhe.de), on quoting the CSD numbers.

Table 2. Fractional atomic coordinates for the three members of the $Ln_4N_2S_3$ series (Ln = Ce–Nd).

Atom	**Site** [1]	**$Ce_4N_2S_3$**		**$Pr_4N_2S_3$**		**$Nd_4N_2S_3$**	
		x/a	***y/b***	***x/a***	***y/b***	***x/a***	***y/b***
$Ln1$	4g	0.22375(5)	0.56460(2)	0.22392(9)	0.56451(3)	0.22374(7)	0.56437(3)
$Ln2$	4g	0.26571(5)	0.84323(2)	0.26709(9)	0.84333(3)	0.26598(8)	0.84315(3)
N	4g	0.1313(7)	0.4154(3)	0.1312(13)	0.4164(6)	0.1312(12)	0.4154(5)
S1	2a	0	0	0	0	0	0
S2	4g	0.2680(2)	0.20004(8)	0.2683(5)	0.20011(16)	0.2636(4)	0.19985(14)

[1] z/c = 0 for all positions.

Table 3. Anisotropic displacement parameters (U_{ij} [1]/pm^2) for the three members of the $Ln_4N_2S_3$ series (Ln = Ce–Nd).

Compound	Atom	U_{11}	U_{22}	U_{33}	U_{23}	U_{13}	U_{12}
$Ce_4N_2S_3$	Ce1	71(2)	51(2)	50(2)	0	0	−4(1)
	Ce2	103(2)	45(2)	46(2)	0	0	−6(1)
	N	96(22)	57(20)	69(20)	0	0	−6(17)
	S1	61(8)	105(9)	69(8)	0	0	−2(7)
	S2	178(7)	55(6)	57(6)	0	0	11(5)
$Pr_4N_2S_3$	Pr1	97(3)	91(3)	59(3)	0	0	−3(2)
	Pr2	140(3)	84(3)	55(3)	0	0	−8(2)
	N	58(38)	138(42)	74(42)	0	0	−5(33)
	S1	119(17)	136(18)	66(16)	0	0	−14(13)
	S2	208(13)	71(11)	81(12)	0	0	29(9)
$Nd_4N_2S_3$	Nd1	111(3)	58(3)	72(3)	0	0	−8(2)
	Nd2	145(3)	54(3)	72(3)	0	0	−9(2)
	N	111(37)	126(40)	93(37)	0	0	−48(31)
	S1	100(14)	95(15)	102(15)	0	0	−11(11)
	S2	223(12)	50(9)	86(10)	0	0	9(8)

[1] Given in the expression $\exp[-2\pi^2(a^{*2}h^2U_{11} + b^{*2}k^2U_{22} + c^{*2}l^2U_{33} + 2b^*c^*klU_{23} + 2a^*c^*hlU_{13} + 2a^*b^*hkU_{12})]$.

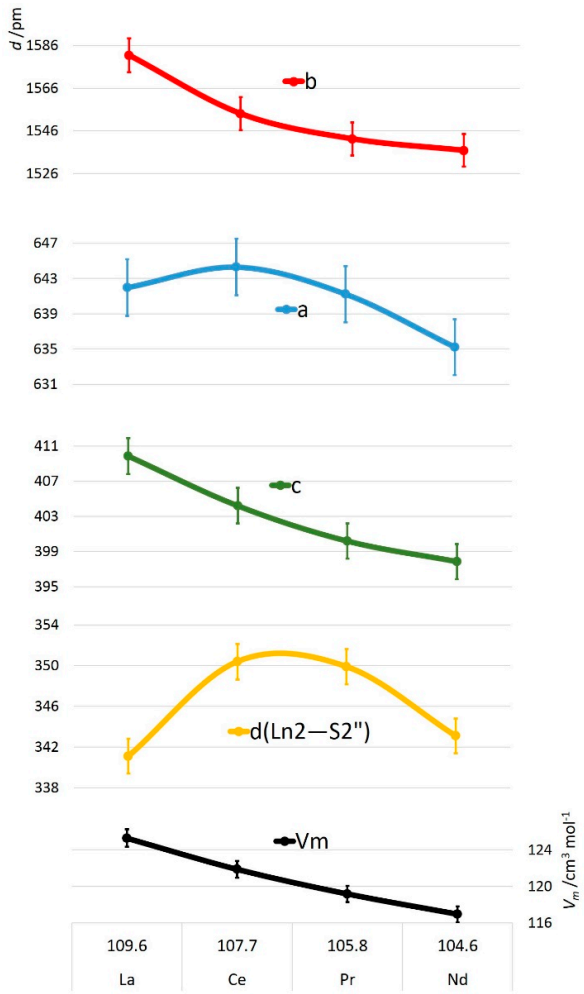

Figure 2. Lattice parameters (a, b, and c), selected distances (d(Ln2–S″)), and molar volumes (V_m) of the complete A-type $Ln_4N_2S_3$ series (Ln = La–Nd, error bars with a percentage of 0.5%) versus the ionic radii (r_i) of the trivalent lanthanide cations [17].

Table 4. Selected interatomic distances (d/pm) and angles ($\measuredangle$/°) for the three members of the $Ln_4N_2S_3$ series (Ln = Ce–Nd) compared to A-type $La_4N_2S_3$.

			La [7]	Ce	Pr	Nd
***Ln*1**	–N	(1×)	233.8(6)	230.9(5)	229.6(9)	227.6(8)
	–N′	(1×)	243.2(6)	239.4(4)	236.1(9)	236.4(8)
	–S1	(2×)	287.8(1)	287.4(1)	285.1(1)	283.1(1)
	–S2	(2×)	296.9(1)	291.9(1)	289.5(2)	288.1(2)
***Ln*2**	–N	(2×)	243.8(3)	240.5(3)	238.7(5)	237.0(5)
	–S1	(1×)	299.8(1)	297.8(1)	296.2(1)	294.4(1)
	–S2	(2×)	306.1(1)	301.4(1)	298.9(2)	297.4(2)
	–S2′	(1×)	315.1(2)	307.9(2)	305.4(3)	306.0(3)
	–S2″	*(1×)*	*341.1(2)*	*350.5(2)*	*349.8(3)*	*342.8(3)*
N	–*Ln*1	(1×)	233.8(6)	230.9(5)	229.6(9)	227.6(8)
	–*Ln*1′	(1×)	243.2(6)	239.4(4)	236.1(9)	236.4(8)
	–*Ln*2	(2×)	243.8(3)	240.5(3)	238.7(5)	237.0(5)
*Ln*1	–**N**–*Ln*1	(1×)	96.3(2)	96.7(2)	97.2(3)	96.5(3)
*Ln*1	–**N**–*Ln*2	(2×)	109.8(2)	109.6(1)	109.4(2)	109.7(2)
*Ln*1	−**N**–*Ln*2′	(2×)	112.5(2)	112.5(1)	112.8(2)	112.7(2)
*Ln*2	–**N**–*Ln*2	(1×)	114.4(2)	114.4(2)	113.9(4)	114.1(3)

In analogy to all the rare-earth metal(III) nitride chalcogenides and their halide derivatives known to date [1–3], the N^{3-} anions are again surrounded by a more or less distorted tetrahedron of Ln^{3+} cations, in which the four N^{3-}–Ln^{3+} distances (228–241 pm) differ by a maximum of 13 pm and the angles range between 97° and 114° (Table 4). In fact, the typical characteristic of the structural construction is actually created by the individual linkage of these $[NLn_4]^{9+}$ tetrahedra. As shown in Figure 3, the $[NLn_4]^{9+}$ units initially occur as dimers $[N_2Ln_6]^{12+}$ by sharing a common edge ($Ln1\cdots Ln1$), and they are then condensed to one-dimensional infinite strands along [001] by corner-linkage (via $Ln2$) with two similar neighboring units corresponding to $^1_\infty\{[N(Ln1)^e_{2/2}(Ln2)^v_{2/2}]^{3+}\}$ (e = edge-linking, v = vertex-linking). This type of $[NLn_4]^{9+}$-tetrahedral linkage is also found in the crystal structures of the nitride chlorides β-Y_2NCl_3 and β-Gd_2NCl_3 [18] and in those of nitride sulfide halides $Ln_6N_3S_4X$ (Ln = La–Nd; X = Cl, Br) [19,20]. In the latter, however, the crystal structure is made up of two kinds of strands that are commensurable with each other along their propagation axis. Figure 4 shows a projection of the crystal structure of the new $Ln_4N_2S_3$ representatives with an A-type $La_4N_2S_3$ structure with a view along the c-axis. The $^1_\infty\{([NLn_2]_2)^{6+}\}$ double strands are separated by two crystallographically different S^{2-} anions with almost octahedral Ln^{3+}-coordination spheres (Table 5). The neighboring cationic chain units in the a-direction are similarly oriented per se, but compared to their adjacent chains in the b-direction, they get mirrored by a diagonal glide plane n that runs vertical to the b-axis at heights of one-fourth and three-fourths and are shifted by one-half in the a- and c-directions, respectively. Thus, a single strand is surrounded by a total of six more in the manner of a hexagonal rod packing.

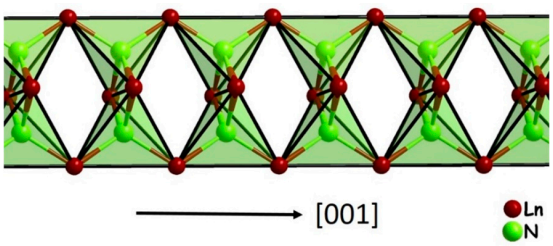

Figure 3. Linkage of tetrahedral $[NLn_4]^{9+}$ units via edges to dimers $[N_2Ln_6]^{12+}$ and their linear vertex connection to $^1_\infty\{[N(Ln1)^e_{2/2}(Ln2)^v_{2/2}]^{3+}\}$ strands along [001] in the crystal structure of the A-type $Ln_4N_2S_3$ series (Ln = La–Nd).

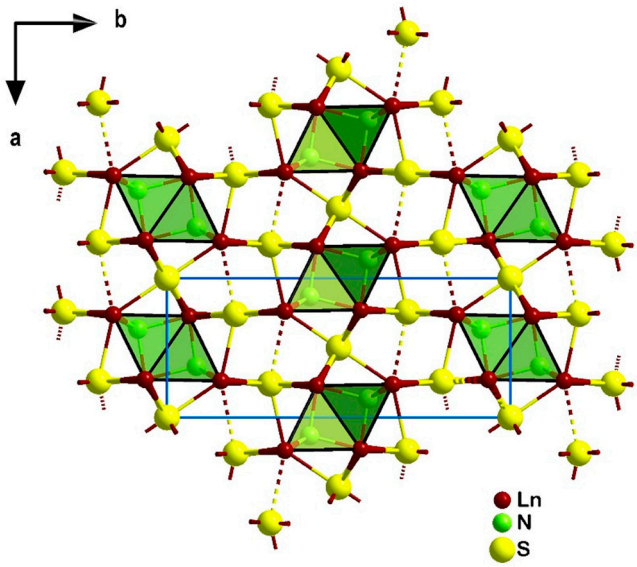

Figure 4. Projection of the crystal structure of the A-type $Ln_4N_2S_3$ series (Ln = La–Nd) on the [001] plane.

Table 5. Motifs of mutual adjunction for the A- and B-type $Ln_4N_2S_3$ structures (Ln = La–Nd).

	***Ln*1**	***Ln*2**	***Ln*3**	***Ln*4**	***C.N.***
		A-type $Ln_4N_2S_3$			
N	2/2	2/2			**4**
S1	2/4	1/2			**6**
S2	2/2	3+1/3+1			**5+1**
C.N.	**6**	**6+1**			
		B-type $Ln_4N_2S_3$			
N1	1/1	1/1	1/1	1/1	**4**
N2	1/1	1/1	1/1	1/1	**4**
S1	1/2	1/2	1/2	0/0	**6**
S2	1/2	0/0	1/2	1/2	**6**
S3	1/1	1/1	1/1	3/3	**6**
S4	1/1	3/3	1/1	1/1	**6**
C.N.	**6**	**7**	**6**	**7**	

Apart from the nitride sulfides $Ln_4N_2S_3$ (Ln = Ce–Nd) and $La_4N_2S_3$ [7] of the orthorhombic A-type modification presented here, a monoclinic form (B-type) for $La_4N_2S_3$ [12] and $Pr_4N_2S_3$ [9] has been reported for each with a crystal structure quite different from the orthorhombic one. Unlike the crystal structure of the A-type $Ln_4N_2S_3$ members (Ln = La, Pr), in which linear chains are built by linkage of $[N_2Ln_6]^{12+}$ bitetrahedra, in the B-type structure layers are produced by their cross-linkage via common vertices according to ${}^{2}_{\infty}\{[N(Ln3/4)^{e}_{2/2}(Ln1/2)^{v}_{2/2}]^{3+}\}$ with four- and eight-fold pores (Figure 5). Accompanied by a quadruplication of the cell volume for the B-type (Z = 8) as compared to the A-type (Z = 2), the unit cell of the B-$Ln_4N_2S_3$ representatives contains four times the total number of cations and anions, but only twice the number of crystallographically different unkind particles owing to the doubling of the respective Wyckoff positions (8*f* and 4*c* or 4*e* as compared to 4*g* and 2*a*). With the exception of the already-mentioned distance Ln2–S2″ which loses its coordinative influence upon the transition from A-$La_4N_2S_3$ to A-$Ce_4N_2S_3$, both kinds of anions (N^{3-} and S^{2-}) as well as the cations can analogously be assigned to each other in their respective modifications as shown in Table 5.

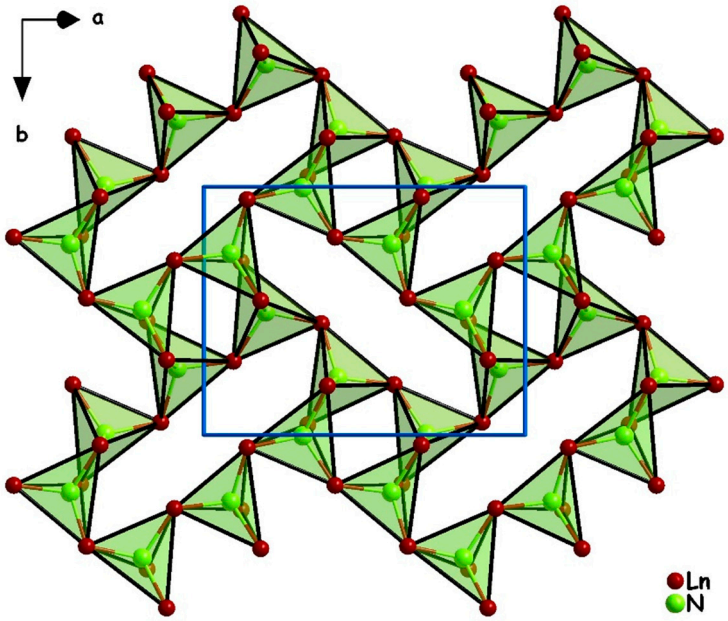

Figure 5. Linkage of tetrahedral $[NLn_4]^{9+}$ units via edges to dimers $[N_2Ln_6]^{12+}$, their initial linear vertex connection to quadruples $[N_4Ln_{10}]^{18+}$ and their final vertex fusion to porous sheets $^{2}_{\infty}\{[NLn_{4/2}]^{3+}\}$ perpendicular to [001] consisting of four- and eight-membered rings in the crystal structure of the B-type $Ln_4N_2S_3$ series (Ln = La, Pr).

In addition to $La_4N_2S_3$ [7,12] crystallizing dimorphously in the A-$La_4N_2S_3$- and in the B-$Pr_4N_2S_3$-type structures and $Ce_4N_2Se_3$, which is observed either with the $Nd_4N_2Se_3$- or with the $Ce_4N_2Te_3$-type arrangement, now the next nitride sulfide of the lanthanoids with the composition $Pr_4N_2S_3$ can represent both the A- and B-type structures. In order to determine the respective high-pressure and/or high-temperature phases, the theoretically calculated densities using X-ray diffraction (D_x) give at least uniform indications, even though they are not strong. With values of 5.426 [7] and 5.772 g/cm^3 (Table 1) the A-type $Ln_4N_2S_3$ members (Ln = La, Pr) show somewhat larger densities as compared to 5.363 [12] and 5.740 g/cm^3 [9], respectively, which are available for the possible low-pressure and/or high-temperature phases of the B-type representatives. To what extent these differences of 1.2% and 0.6% could be significant is left to the reader to determine. As the physical parts of the preparation methods for members of both modifications are identical (seven days at 900 °C in evacuated fused silica ampoules, see Experimental), only the chemical conditions can provide an explanation. If for the synthesis of the A-type $Ln_4N_2S_3$ representatives (Ln = La–Nd), in addition to the lanthanoid metal and sulfur, cesium azide (CsN_3) and the corresponding lanthanide bromide ($LnBr_3$, Ln = La–Nd) with CsBr as a fluxing agent were used (see Experimental), the alkali metal and the halides in the form of the triiodides LnI_3 (Ln = La, Pr), sodium azide (NaN_3) and fluxing NaI varied for the preparation of the B-type $Ln_4N_2S_3$ ones. Whether, in this case, the intermediates formed, such as elemental iodine (causing changes in pressure or chemical transport) or ternary halides (such as Cs_3LnBr_6 [21] in the first or Na_3LnI_6 [22] in the second case) play a role can only be speculated.

3. Experimental

As adapted from the standard methodology reported in [1], the new lanthanoid nitride sulfides $Ln_4N_2S_3$ (Ln = Ce–Nd) are obtained by the reaction of lanthanoid metal (Ln; ChemPur: 99.9%) with sulfur (S; ChemPur: 99.9999%) and lanthanoid tribromide ($LnBr_3$; prepared from CeO_2, Pr_6O_{11} and Nd_2O_3 (all: Johnson-Matthey: 99.999%) by the ammonium-bromide method [23]) and cesium azide (CsN_3; Ferak: 99.9%). On adding cesium bromide (CsBr; ChemPur: 99.9%) as flux almost black, rod-shaped single crystals of the target compounds $Ln_4N_2S_3$ (Ln = Ce–Nd) that reflect strongly in the

incident light under a microscope are obtained after seven days at 900 °C in evacuated torch-sealed fused silica tubes.

Nonetheless, the process of the reaction according to

$$34\ Ln + 27\ S + 6\ CsN_3 + 2\ LnBr_3 \rightarrow 9\ Ln_4N_2S_3 + 6\ CsBr\ (Ln = \text{Ce–Nd}),$$

which can be classified as redox metathesis with the formation of CsBr as driving force, is *not* complete. Besides some white amorphous parts, which are presumably produced by undesired reactions with the silica-ampoule walls, mostly brown rods that could be characterized as Ln_3NS_3 representatives (Ln = Ce–Nd) [24] were also obtained. As in addition to this the whole product mixture in excess of CsBr is stable to hydrolysis, so the fluxing agent and by-product can easily be rinsed off with water. A largest possible black rod ($0.02 \times 0.03 \times 0.20$ mm^3) of each of the new $Ln_4N_2S_3$ members was selected from the mixture under paraffin oil and transferred into a mark-tube capillary to subsequently record the intensity data sets of X-ray diffraction experiments with the help of a plate detector (four-circle diffractometer Kappa-CCD, Bruker AXS). In Tables 1–3 the crystallographic data for the three new nitride sulfides $Ln_4N_2S_3$ (Ln = Ce–Nd) are summarized.

4. Conclusions

The new series of lanthanoid(III) nitride sulfides with the composition $Ln_4N_2S_3$ (Ln = Ce–Nd) adopting the A-type structure of $La_4N_2S_3$ [7] expands the knowledge about the constitution of lanthanoid(III) nitride chalcogenides in general. Just like for all members of the formula types Ln_3NCh_3 [2,24] and $Ln_4N_2Ch_3$ [4–12], nitride-centered lanthanoid tetrahedra $[NLn_4]^{9+}$ display the fundamental building units, which are here connected by one edge (e) and two vertices (v) each to form $^1_\infty\{([N(Ln1)^e_{2/2}(Ln2)^v_{2/2}]^{3+})_2\}$ chains. Bundled like hexagonal rod packing, they are held together by S^{2-} anions taking care of the charge compensation. Whereas the coordination numbers (*C.N.* = 5–6) of these compare well with those in the binary sesquisulfides Ln_2S_3 with A- or C-type crystal structures (*C.N.* = 5–6) [25–29], the presence of tetrahedrally coordinated N^{3-} anions baffles a little, since all binary lanthanoid(III) mononitrides LnN [30,31] exhibit octahedrally coordinated N^{3-} anions in their rocksalt-type crystal structures.

Supplementary Materials: The following are available online at www.mdpi.com/2304-6740/5/1/2/s1, cif and checkcif files of $Ce_4N_2S_3$, $Nd_4N_2S_3$, and $Pr_4N_2S_3$.

Acknowledgments: At this point the authors gratefully acknowledge the *State of Baden-Württemberg* (Stuttgart, Germany), the *Deutsche Forschungsgemeinschaft* (Bonn, Germany) and the *Fonds der Chemischen Industrie* (Frankfurt am Main, Germany) for considerable financial support.

Author Contributions: Falk Lissner conceived and performed the experiments; Falk Lissner recorded the intensity data sets of X-ray diffraction experiments and analyzed the data; Falk Lissner and Thomas Schleid wrote the paper.

Conflicts of Interest: The authors declare no conflict of interest.

References

1. Schleid, T.; Lissner, F. Lanthanido ammonium cations $[NM_4]^{9+}$ as main structural features in lanthanide(III) nitride chalcogenides and their derivatives. *J. Alloys Compd.* **2008**, *451*, 610–616. [CrossRef]
2. Schurz, C.M.; Talmon-Gros, P.; Lissner, F.; Schleid, T. The gadolinium nitride selenides Gd_3NSe_3 and $Gd_{23}N_5Se_{27}$: Three connectivity types of $[NGd_4]^{9+}$ tetrahedral and fivefold coordinated Gd^{3+} cations. *Solid State Sci.* **2013**, *17*, 140–145. [CrossRef]
3. Foltin, M.L.; Lissner, F.; Schleid, T. Renaissance of the Stella Quadrangula: Lanthanide(III) Nitride Tellurides $Ln_{13}N_5Te_{12}$ (Ln = La–Nd). *Eur. J. Inorg. Chem.* **2017**. in progress.
4. Lissner, F.; Schleid, T. Ein neues Samariumnitridsulfid: $Sm_4N_2S_3$. *Z. Anorg. Allg. Chem.* **1994**, *620*, 2003–2007. [CrossRef]
5. Lissner, F.; Schleid, T. $M_4N_2Te_3$ (M = La–Nd): Die ersten Nitridtelluride der Lanthanide. *Z. Anorg. Allg. Chem.* **2005**, *631*, 1119–1124. [CrossRef]

6. Foltin, M.L.; Lissner, F.; Strobel, S.; Schleid, T. A group-subgroup relationship between the new nitride tellurides of terbium and dysprosium with the composition $M_4N_2Te_3$. *Z. Anorg. Allg. Chem.* **2014**, *640*, 1247–1253. [CrossRef]
7. Lissner, F.; Schleid, T. $La_4N_2S_3$: Ein neues Nitridsulfid des Lanthans mit beispielloser Kristallstruktur. *Z. Anorg. Allg. Chem.* **2006**, *632*, 1167–1172. [CrossRef]
8. Lissner, F.; Schleid, T. $Nd_4N_2Se_3$ und $Tb_4N_2Se_3$: Zwei nicht-isotype Lanthanoid(III)-Nitridselenide. *Z. Anorg. Allg. Chem.* **2003**, *629*, 1027–1032. [CrossRef]
9. Lissner, F.; Schleid, T. $Pr_4N_2S_3$ und $Pr_4N_2Se_3$: Zwei *nicht*-isotype Praseodym(III)-Nitridchalkogenide. *Z. Anorg. Allg. Chem.* **2005**, *631*, 427–432. [CrossRef]
10. Lissner, F.; Schleid, T. Dimorphic $Ce_4N_2Se_3$ with orthorhombic $Ce_4N_2Te_3$- and monoclinic $Nd_4N_2Se_3$-type structure. *Z. Krist.* **2011**, *S31*, 1595.
11. Lissner, F.; Schleid, T. Coming first: The lanthanum nitride selenide $La_4N_2Se_3$ with monoclinic $Nd_4N_2Se_3$-type crystal structure. *Z. Anorg. Allg. Chem.* **2012**, *638*, 1167–1172. [CrossRef]
12. Lissner, F.; Schleid, T. B-$La_4N_2S_3$: A Second Modification of Lanthanum(III) Nitride Sulfide. *Z. Anorg. Allg. Chem.* **2016**, *642*, 1038.
13. Hoppe, R. Effective Coordination Numbers (ECoN) and Mean Fictive Ionic Radii. *Z. Krist.* **1979**, *150*, 23–52. [CrossRef]
14. Herrendorf, W.; Bärnighausen, H. *HABITUS*, Version 1.06; Program for the Optimization of the Crystal Shape for Numerical Absorption Correction in X-SHAPE; Fa. Stoe: Darmstadt, Germany, 1999; Karlsruhe, Germany, 1993; Gießen, Germany, 1996.
15. Sheldrick, G.M. *SHELX-97*: Program Package for the Solution and Refinement of Crystal Structures from X-ray Diffraction Data, Göttingen 1997. *Acta Crystallogr.* **2008**, *A64*, 112–122. [CrossRef] [PubMed]
16. Prince, E. (Ed.) *International Tables for Crystallography, Vol. C*, 3rd ed.; Springer: Dordrecht, The Netherlands, 2004.
17. Shannon, R.D. Revised Effective Ionic Radii and Systematic Studies of Interatomic Distances in Halides and Chalcogenides. *Acta Crystallogr.* **1976**, *A32*, 751–767. [CrossRef]
18. Meyer, H.-J.; Jones, N.L.; Corbett, J.D. A New Yttrium Sesquichloride Nitride, β-Y_2Cl_3N, That Is Isostructural with the Binary Yttrium Sesquichloride. *Inorg. Chem.* **1989**, *28*, 2635–2637. [CrossRef]
19. Lissner, F.; Meyer, M.; Schleid, T. Nitridsulfidchloride der Lanthanide: II. Der Formeltyp $M_6N_3S_4Cl$ (M = La–Nd). *Z. Anorg. Allg. Chem.* **1996**, *622*, 275–282. [CrossRef]
20. Lissner, F.; Schleid, T. Nitridsulfidhalogenide leichten Lanthanide vom Typ $M_6N_3S_4X$ (M = La–Nd; X = Cl, Br) mit ausgeordneten Sulfid- und Halogenid-Lagen. *Z. Naturforsch.* **2002**, *57b*, 1079–1084.
21. Gundiah, G.; Brennan, K.; Yan, Z.; Samulon, E.C.; Wu, G.; Bizarri, G.A.; Derenzo, S.E.; Bourret-Courchesne, E.D. Structure and scintillation properties of Ce^{3+}-activated $Cs_2NaLaCl_6$, Cs_3LaCl_6, $Cs_2NaLaBr_6$, Cs_3LaBr_6, Cs_2NaLaI_6 and Cs_3LaI_6. *J. Lumin.* **2014**, *149*, 374–384. [CrossRef]
22. Bohnsack, A.; Meyer, G. Ternäre Halogenide vom Typ A_3MX_6. V. Synthese, Kristallstrukturen und Natrium-Ionenleitfähigkeit der ternären Iodide Na_3MI_6 (M = Sm, Gd–Dy) sowie der Mischkristalle $Na_3GdBr_{6-x}I_x$. *Z. Anorg. Allg. Chem.* **1997**, *623*, 837–843. [CrossRef]
23. Meyer, G.; Dötsch, S.; Staffel, T. The Ammonium-Bromide Route to Anhydrous Rare Earth Bromides, MBr_3. *J. Less Common Met.* **1987**, *127*, 155–160. [CrossRef]
24. Lissner, F.; Meyer, M.; Kremer, R.K.; Schleid, T. M_3NS_3 (M = La–Nd, Sm, Gd–Dy): Struktur und Magnetismus von 3:1:3-Typ-Nitridsulfiden dreiwertiger Lanthanide. *Z. Anorg. Allg. Chem.* **2006**, *632*, 1995–2002. [CrossRef]
25. Besançon, P.; Adolphe, C.; Flahaut, J.; Laruelle, P. Sur les varietes alpha et beta des sulfures L_2S_3 des terres rares. *Mater. Res. Bull.* **1968**, *615*, 19–26.
26. Schleid, T.; Lissner, F. Einkristalle von A-Nd_2S_3, U-Ho_2S_3, D-Er_2S_3 und E-Lu_2S_3 durch Oxidation reduzierter Chloride der Lanthanide mit Schwefel. *Z. Anorg. Allg. Chem.* **1992**, *615*, 19–26. [CrossRef]
27. Schleid, T.; Lissner, F. A-Pr_2S_3, D-Ho_2S_3 und E-Yb_2S_3: Synthese und Einkristalluntersuchungen. *Z. Naturforsch.* **1996**, *51b*, 733–738.
28. Schleid, T.; Lauxmann, P. Röntgenstrukturanalysen an Einkristallen von Ce_2S_3 im A- und C-Typ. *Z. Anorg. Allg. Chem.* **1999**, *625*, 1053–1055. [CrossRef]
29. Lauxmann, P.; Strobel, S.; Schleid, T. Einkristalle von $CuPrS_2$ im A- und Pr_2S_3 im C-Typ bei Versuchen zur Synthese ternärer Kupfer(I)-Praseodym(III)-Sulfide. *Z. Anorg. Allg. Chem.* **2002**, *628*, 2403–2408. [CrossRef]

30. Klemm, W.; Winkelmann, G. Zur Kenntnis der Nitride der Seltenen Erdmetalle. *Z. Anorg. Allg. Chem.* **1956**, *288*, 87–90. [CrossRef]
31. Von Essen, U.; Klemm, W. Zur Kenntnis der Nitride der Cererden. *Z. Anorg. Allg. Chem.* **1962**, *317*, 25–34. [CrossRef]